Am. J. Hum. Genet. 74:721–730, 2004

Report

Mutations in *LRP5* or *FZD4* Underlie the Common Familial Exudative Vitreoretinopathy Locus on Chromosome 11q

Carmel Toomes,[1] Helen M. Bottomley,[1] Richard M. Jackson,[2] Katherine V. Towns,[1] Sheila Scott,[1] David A. Mackey,[3] Jamie E. Craig,[3,4] Li Jiang,[5] Zhenglin Yang,[5] Richard Trembath,[6] Geoffrey Woodruff,[7] Cheryl Y. Gregory-Evans,[8] Kevin Gregory-Evans,[8] Michael J. Parker,[9] Graeme C. M. Black,[10,11] Louise M. Downey,[1] Kang Zhang,[5] and Chris F. Inglehearn[1]

[1]Molecular Medicine Unit and [2]School of Biochemistry and Molecular Biology, University of Leeds, Leeds; [3]Centre for Eye Research Australia, Royal Victorian Eye and Ear Hospital, Melbourne; [4]Department of Ophthalmology, Flinders Medical Centre, Adelaide; [5]Department of Ophthalmology & Visual Science and Program in Human Molecular Biology and Genetics, University of Utah, Salt Lake City; Departments of [6]Clinical Genetics and [7]Ophthalmology, Leicester Royal Infirmary, University of Leicester, Leicester, United Kingdom; [8]Faculty of Medicine, Imperial College, London; [9]Sheffield Children's Hospital, Sheffield, United Kingdom; [10]Academic Unit of Ophthalmology, University of Manchester, Manchester Royal Eye Hospital, and [11]University Department of Medical Genetics and Regional Genetics Service, St. Mary's Hospital, Manchester, United Kingdom

Familial exudative vitreoretinopathy (FEVR) is an inherited blinding disorder of the retinal vascular system. Autosomal dominant FEVR is genetically heterogeneous, but its principal locus, *EVR1*, is on chromosome 11q13-q23. The gene encoding the Wnt receptor frizzled-4 (*FZD4*) was recently reported to be the *EVR1* gene, but our mutation screen revealed fewer patients harboring mutations than expected. Here, we describe mutations in a second gene at the *EVR1* locus, low-density-lipoprotein receptor–related protein 5 (*LRP5*), a Wnt coreceptor. This finding further underlines the significance of Wnt signaling in the vascularization of the eye and highlights the potential dangers of using multiple families to refine genetic intervals in gene-identification studies.

Familial exudative vitreoretinopathy (FEVR [MIM 133780]) is a well-defined inherited disorder of retinal vessel development (Benson 1995). It is reported to have a penetrance of 100%, but clinical features can be highly variable, even within the same family. Severely affected patients may be legally blind during the 1st decade of life, whereas mildly affected individuals may not even be aware of symptoms and may receive a diagnosis only by use of fluorescein angiography (Ober et al. 1980). The primary pathological process in FEVR is believed to be a premature arrest of retinal angiogenesis/vasculogenesis or retinal vascular differentiation, leading to incomplete vascularization of the peripheral retina (van Nouhuys 1991). This failure to vascularize the peripheral retina is the unifying feature seen in all affected individuals, but, by itself, it usually causes no clinical symptoms. The visual problems in FEVR result from secondary complications due to the development of hyperpermeable blood vessels, neovascularization, and vitreoretinal traction (fig. 1). These features cause a reduction in visual acuity and, in 20% of cases, can lead to partial or total retinal detachment (van Nouhuys 1991).

FEVR is genetically heterogeneous, with autosomal dominant (Gow and Oliver 1971; Laqua 1980), X-linked (Plager et al. 1992; Shastry et al. 1997*a*), and autosomal recessive (Shastry and Trese 1997*b*; De Crecchio et al. 1998) modes of inheritance described, with autosomal dominant inheritance being the most common (Müller et al. 1994; Shastry et al. 2000; Kondo et al. 2001). To date, two autosomal dominant loci have been mapped. *EVR1* on chromosome 11q was the first FEVR locus to be identified (Li et al. 1992*a*), and, subsequently, other groups have published further families with *EVR1* linkage (Li et al. 1992*b*; Müller et al. 1994; Price et al. 1996; Shastry et al. 2000; Kondo et al. 2001), suggesting that mutations

Received November 14, 2003; accepted January 15, 2004; electronically published March 11, 2004.

Address for correspondence and reprints: Dr. Carmel Toomes, Molecular Medicine Unit, Level 6, Clinical Sciences Building, St. James's University Hospital, Leeds LS9 7TF, United Kingdom. E-mail: c.toomes@leeds.ac.uk

0002-9297/2004/7404-0012$15.00

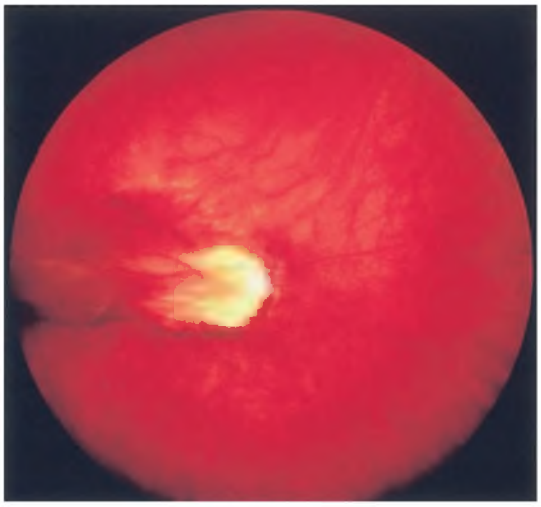

Figure 1 Clinical appearance of FEVR. Fundus photograph shows a fold of retinal tissue due to vitreoretinal traction originating from the temporal periphery. This obscures the posterior pole of the right eye and therefore compromises the visual acuity.

at this locus are a common cause of FEVR. A second dominant locus, *EVR3* on chromosome 11p, has also been described in a single large pedigree (Downey et al. 2001). Although the gene underlying *EVR3* remains unidentified, the gene encoding the Wnt receptor frizzled-4, *FZD4* (MIM 604579), was recently reported as the *EVR1* gene (Robitaille et al. 2002).

Following the identification of *FZD4* mutations in patients with FEVR, we screened an FEVR patient panel of 40 index cases for mutations in this gene. Although we did find mutations, confirming the results of Robitaille et al. (2002), these were identified in only eight (20%) patients (Toomes et al., in press). A similar low number of mutations was reported by Robitaille et al. (2002), who identified mutations in two (40%) of the five families they screened, and a recent study by Kondo et al. (2003) also identified mutations in only 5 (20%) of 24 probands screened. These results are inconsistent with previous reports suggesting that *EVR1* is the common locus for autosomal dominant FEVR (Müller et al. 1994; Price et al. 1996; Shastry et al. 2000; Kondo et al. 2001). Moreover, our screen also revealed the absence of a mutation in a family with proven *EVR1* linkage (Price et al. 1996). To investigate this family further, we analyzed the linked haplotype in the *EVR1* region of chromosome 11q13, and we found that crossovers refined the disease gene in this family to an interval of ~15 cM between the markers D11S1368 and D11S937, 10 cM centromeric to *FZD4*. These data strongly suggested the presence of a second gene mutated in FEVR, close to *FZD4* and within the previously defined *EVR1* locus (Toomes et al. 2004).

Despite the fact that >250 genes are located within the defined interval, the discovery that FEVR can be caused by mutations in the Wnt receptor FZD4 highlighted proteins involved in the Wnt-signaling pathway as candidate FEVR genes (for an up-to-date list of all the proteins involved in Wnt signaling, see the Wnt Gene Homepage maintained by the Roel Nusse lab). We identified *LRP5* (MIM 603506) as one such candidate gene in the region. *LRP5* and its closely related homologue *LRP6* encode single-pass transmembrane receptors that partner with members of the frizzled family of seven-pass transmembrane receptors to bind Wnt proteins, forming a functional ligand-receptor complex that activates the canonical Wnt-β-catenin pathway (Pinson et al. 2000; Tamai et al. 2000; Wehrli et al. 2000). *LRP5* consists of 23 exons and encodes a 1,615–amino acid protein. Its extracellular segment contains four domains, each composed of six YWTD repeats (which form a β-propeller structure) and an epidermal growth factor–like domain (YWTD-EGF domain). These are followed by three low-density-lipoprotein receptor–like (LDL-R–like) ligand-binding domains (fig. 2). The specific function of LRP5 remains unknown, but loss of this protein causes osteoporosis-pseudoglioma syndrome (OPPG [MIM 259770]), a recessive disorder characterized by very low bone mass and blindness (Gong et al. 2001). Individuals with OPPG are

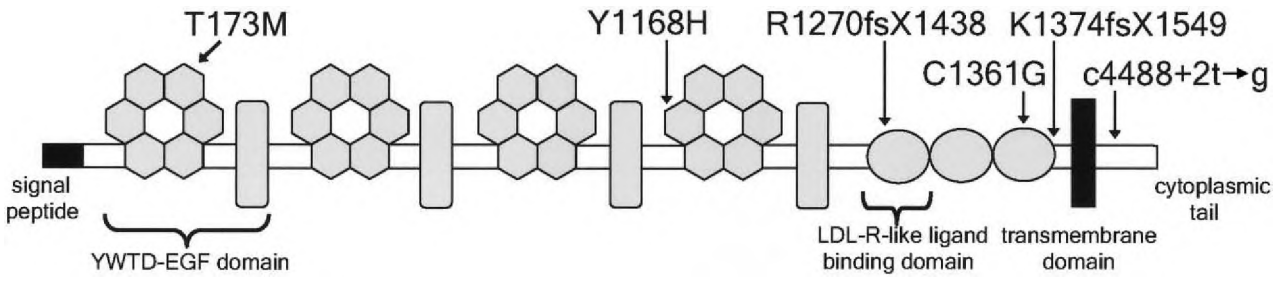

Figure 2 Schematic diagram of the LRP5 protein showing the location of the mutations within the protein domains. The six YWTD repeats are shown as a hexagon to represent their β-propeller structure, whereas the EGF domains are represented as gray blocks.

prone to developing bone fractures and deformations and can have various eye abnormalities, including phthisis bulbi, retinal detachments, falciform folds, or persistent vitreal vasculature (Frontali et al. 1985). Dominant missense mutations in *LRP5* have also been described in patients with high-bone-mass disorders (high bone mass [MIM 601884], endosteal hyperostosis [MIM 144750], and osteopetrosis [MIM 607634]) (Boyden et al. 2002; Little et al. 2002; Van Wesenbeeck et al. 2003). It is thought that these missense mutations result in the formation of a mutant LRP5 protein that is functionally abnormal (Boyden et al. 2002).

In light of these findings, *LRP5* was a strong candidate for involvement in FEVR and was therefore screened in the remaining 32 patients from our FEVR patient panel. Informed consent was obtained from all subjects tested, and ethical approval was obtained from the Leeds Teaching Hospitals Trust research ethics committee. We designed primers (table 1) and screened all 23 exons and flanking intronic sequences by SSCP-heteroduplex analysis (SSCP-HA) and direct sequencing, using established protocols (Toomes et al. 2001). In total, we discovered six *LRP5* mutations not present in control individuals (figs. 2 and 3) and a further 13 benign sequence variants not previously described (table 2).

We first identified a splice-donor mutation that segregated with FEVR in the family with *EVR1* linkage in which *FZD4* mutations had been excluded by genetics (fig. 3*B* [family 1]). This mutation is a substitution of the second nucleotide of intron 21, changing the GT splice-donor site to GG, c4488+2t→g. The precise effect of this mutation has not been determined in this family, since no RNA was available. However, the most common outcome of splice-donor mutations is the deletion of the preceding exon. This would lead to the deletion of exon 21, resulting in a frameshift after codon 1449, followed by 52 incorrect amino acids and a premature termination at codon 1502.

In a second family originating from the United States, we identified a 1-bp insertion in exon 20, c4119-4120insC. This mutation segregates with the disease in that family but was also found in two asymptomatic family members (fig. 3*B* [family 2]). However, neither of these individuals had been examined by fluorescein angiog-

Table 1

***LRP5* SSCP-HA Primers**

Exon[a]	Primer Name	5′→3′ Sequence	Primer Name	5′→3′ Sequence	Size (bp)
1	A1F[b]	TTCCGCTCCCGCGCGCCCAGCT	1R2[b]	GCGGGGCCGCCCGGGCCATT	311
2 start	2F[b]	CATCCCAGGGCTGTGTATCT	SSCP 2-R	GTGATGACCACGTTCTGCAC	288
2 end	SSCP 2-F	CAAGCAGACCTACCTGAACC	2R[b]	ACTTGGGCTCATGCAAATTC	309
3 start	3F3[b]	GAAACCATACCTGTTGGTTATTTCC	SSCP 3-R	GGATGAAGCTGAGCTTGGCGTC	311
3 end	SSCP 3-F	CGGATTGAGCGGGCAGGGAT	3R3[b]	CACAGACCCTGACGCTGTTC	323
4	4F4[b]	GATGGCTCCTCCACCCCGCT	4R5[b]	GCGCCCCAGCCGGCACT	250
5	5F3[b]	CTCATTCAGAAACAAGTGACGGTCCTC	5R4[b]	GTCCCGTCCCACCGCCT	216
6 start	6F1[b]	TGGCTGAGTATTTCCCTTGCCC	SSCP 6-R	GTCGACCGCGATGCCATCGG	352
6 end	SSCP 6-F	CGACCCGCTAGAGGGCTATGT	SSCP 6-2R	CAATCTCCCTCTCGCCTGTGC	338
7	7F[b]	GATGCTGCAGAGACCAGACA	7R2[b]	TAACTATTTTCTCAAGCATTCCATGT	366
8 start	8F1[b]	TGAAGTTGCTGCTCTTGGGCA	SSCP 8-R	CACCCGCTCGATGCTGCGGC	256
8 end	SSCP 8-F	CGCACATTTTCGGGTTCACGC	8R1[b]	AACACTTATGCCCAGGCATGGA	252
9 start	9F1[b]	TGCTGGGCTGTTGATGTTTAGACT	SSCP 9-R	CCGTGAGCGGGATGGCCACG	263
9 end	SSCP 9-F	GTGCCTGAGGCCTTCTTGGTCT	9R1[b]	CTTGAACTGCGTTACAATAAATACGA	291
10	10F1[b]	GATGCTGGTTCCTAAAATGTGG	10R[b]	GCTCTAATCACTGAGGGCCA	386
11	11F1[b]	GAGGGCTGAGCTGAAGAGGT	11R1[b]	CAGGTTGGGGAACTTGCAG	398
12 start	12F[b]	ATTCATGTGGTCGCTAGGCT	SSCP 12-R	CATCACGAAGTCCAGGTGG	281
12 end	SSCP 12-F	CTAGCGGCCGGAACCGCA	12R[b]	GAAGCTCCTTTCAGCGTCAG	287
13	13F[b]	CCAGCTCCTCTGTGGCTTAC	13R[b]	TCCTCCCTCTGCTAAGGACA	352
14	SSCP 14-F	GTCTCCGCCAGTGCTCAG	SSCP 14-R	CTGTGAGAGGCTGGCATTC	334
15	SSCP 15-F	GTGCTGTCCGAGGAGACGC	15R2[b]	TTACTGACAATGAAGGCCGGGT	305
16	16F1[b]	AAGCTGAGTGTGGGGCAAGTTC	SSCP 16-R	CCACACAGGATCTTGCACTGG	361
17	17F[b]	CATGAGTTCTCATTTGGCCC	17R[b]	GCCACAGGGACTGTGATTTT	321
18	SSCP 18-F	GGCTGCGTGTGATGTTCTC	18R[b]	CAGAGCCCCTACTCCTGTGA	371
19	19F[b]	CCAGACCTTGGTTGCTGTG	19R[b]	CGTCTCCTCCCCTAAACTCC	269
20	20NF[b]	ATGTTGGCCACCTCTTTCTG	20NR[b]	CTGCCTCCTCCAGATCATTC	310
21	21F[b]	GAGTCTCGTGGGTAGTGGGA	SSCP 21-R	AGAAAGCAAGCATGCCTCAGAG	373
22	S22F[b]	GGAGGAAGGAAGGAATGCCC	22R[b]	GCCCACTAGCACCCAGAATA	272
23	SSCP 23-F	CGGATGTGCCTACCGAATC	SSCP 23-R	TTACAGGGGCACAGAGAAGC	347

[a] Large exons were amplified in two overlapping segments, designated "start" and "end."

[b] Primer sequences obtained from Gong et al. (2001).

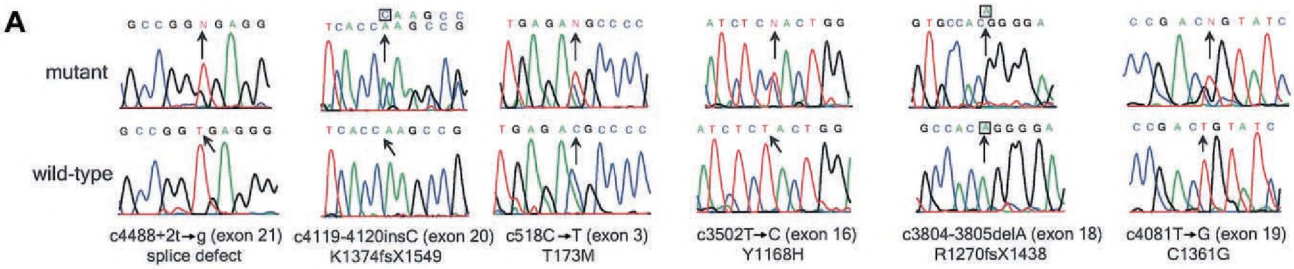

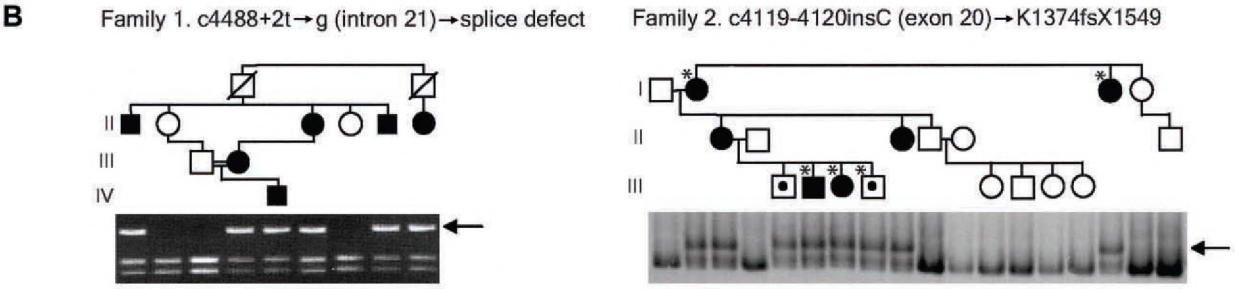

C

T173M

```
hLRP5     163 GYMYWTDWGETPRIERAGMDG--S--TR 183
mLRP5     162 GYMYWTDWGEAPRIERAGMDG--S--TR 182
xLRP5     151 GYMYWTDWGETPRIERAGMDG--S--TR 171
hLRP6     150 GFMYWTDWGEVPKIERAGMDG--S--SR 170
mLRP6     150 GFMYWTDWGEVPNIERAGMDG--S--SR 170
xLRP6     150 GYMYWTDWGEVPKIERAGMDG--S--VR 170
arrow     225 KLLIWTDWGEYPKIERASMDG--DPLSR 245
mosquito  192 RYMIWTDWGESPKIERASMDGDPQ--SR 212
hLRP4     196 GTIYWTDWGNTPRIEASSMDG--S--GR 216
```

Y1168H

```
hLRP5    1156 QPLGLTILGKHLYWIDRQQQM 1176
mLRP5    1155 QPVGLTVLGRHLYWIDRQQQM 1175
xLRP5    1148 QPMGLTILGDYLYWIDKQQQM 1168
hLRP6    1146 QPVGLTVFENWLYWIDKQQQM 1166
mLRP6    1146 QPVGLTVFENWLYWIDKQQQM 1166
xLRP6    1145 QPVGLTVFGNYLYWIDRQQQM 1165
arrow    1214 QVINIAALGGFVYWLD-DKTG 1233
arrow     302  YPFSLTFYDDRLYWTDWQRGS 322
mosquito 1192 MVSSIAALDGFIYWLD-ERPV 1211
hLRP4    1188 HPFALTQQDRWIYWTDWQTKS 1208
```

C1361G

```
hLRP5    1348 CVLIKQQCDSFPDCIDGSDE 1367
mLRP5    1347 CVLIKQQCDSFPDCADGSDE 1366
xLRP5    1340 CIMTSQQCDTFPDCSDSSDE 1359
hLRP6    1338 CIGKHKKCDHNVDCSDKSDE 1357
mLRP6    1338 CVGKHKKCDHSVDCSDRSDE 1357
xLRP6    1338 CIGKHRRCDLSPDCSDSSDE 1357
arrow    1414 CISAALLCDGWENCADGADE 1433
mosquito 1392 CISFHNVCDGDEHCAKGEDE 1411
```

raphy to exclude a very mild phenotype, so their undiagnosed condition was not unexpected (Ober et al. 1980). This mutation causes a frameshift resulting in 175 incorrect amino acids after codon 1373, followed by a premature termination at codon 1549 (K1374fsX1549). The third mutation identified was a 1-bp deletion in exon 18, c3804delA, in a single Indian patient. This mutation causes a frameshift resulting in the substitution of 168 amino acids after codon 1269 and a premature stop in codon 1438 (R1270fsX1438).

The remaining three potential mutations were missense changes. In exon 3, we identified T173M (c518C→T) in an elderly British woman with abnormal retinal vasculature and retinal folds. In exon 16, we identified Y1168H (c3502T→C) in a British woman with a total retinal detachment and retinoschisis. The patient was born after 36 wk of pregnancy but was never treated with oxygen therapy. The patient had no family history of FEVR, although the patient's asymptomatic father was also found to have the mutation. The final mutation, C1361G (c4081T→G), was identified in exon 19 in a 6-year-old Australian boy with classic features of FEVR. This patient has very poor vision and has undergone surgery on his left eye, which is phthisical and sunken. There is no family history of FEVR, but, again, the asymptomatic mother was found to have the mutation. Neither of the asymptomatic parents had been examined by fluorescein angiography, but they showed no signs of retinopathy upon fundus examination. To exclude the possibility that these changes were common polymorphisms, we screened 200 ethnically matched control individuals (400 chromosomes) for each of these changes (Collins and Schwartz 2002). We also checked each of the mutated amino acids for conservation within homologues of LRP5 from human and other species (fig. 3C). Both Y1168H and C1361G are changes to highly conserved residues. T173M is not well conserved, although the methionine residue at this position is not seen in any FZD4 homologue in another species. Whereas these results suggest that these missense changes are indeed pathogenic, without further examination by means of a functional assay, we are unable to prove categorically that they are disease-causing mutations.

Table 2

Summary of Novel Benign Sequence Variants Detected in *LRP5*

Location	cDNA Change	Protein Change	Frequency
Exon 2	324C→G	V108V	C 98%; G 2%
Intron 2	488+53t→c	...	t 52%; c 48%
Exon 3	639C→T	D213D	C 98%; T 2%
Intron 3	686+61c→t	...	c 99%; t 1%
Intron 8	1801+62 c→t	...	c 99%; t 1%
Intron 11	2503+37 c→t	...	c 99%; t 1%
Intron 11	2503+78 g→a	...	g 52%; a 48%
Exon 18	3918G→A	A1306A	G 99%; A 1%
Intron 20	4348+13a→g	...	a 99%; g 1%
Exon 21	4380C→T	S1460S	C 98%; T 2%
Exon 21	4431C→T	H1477H	C 98%; T 2%
Intron 21	4488+54c→a	...	c 99%; a 1%
Intron 21	4488+58g→a	...	g 98%; a 2%
Exon 22	4574T→C	V1525A	T 99%; C 1%

NOTE.—Amino acid and nucleotide numbering follows the cDNA sequence, with nucleotide position 1 assigned to the first nucleotide of the ATG initiation codon in exon 1. Bases in exons are denoted by uppercase letters, bases in introns by lowercase letters. (NCBI assay ID numbers for these SNPs appear in the dbSNP entry of the "Electronic-Database Information" section.)

On the basis of these results, we propose that FEVR results from heterozygous mutations that cause haploinsufficiency of LRP5. The insertion, deletion, and splicing mutations all lead to transcripts with premature termination, which are likely to be targeted by nonsense-mediated decay. Similar mutations, when homozygous, cause OPPG. Indeed, c3804delA has been reported elsewhere as a homozygous mutation in a patient with OPPG (Gong et al. 2001). It is therefore likely that the missense mutations identified also knock out the function of LRP5. In support of this theory, the C1361G mutation, which affects the fifth cysteine within the third LDL-R–like ligand-binding domain, is an invariant cysteine required to form a disulfide bond necessary for correct protein folding (Bieri et al. 1995; Fass et al. 1997).

The remaining two missense mutations identified in patients with FEVR occur within the first and fourth YWTD-EGF domains (fig. 2). To determine the functional significance of these mutations, we constructed a model of the YWTD-EGF domain 1 of LRP5 based on the

Figure 3 FEVR caused by mutations in *LRP5*. *A*, Sequence traces of the six mutations identified and the corresponding wild-type alleles. The mutation-sequence trace for exon 18 was obtained from a cloned PCR product, so only the disease allele is shown. Other mutations were identified from directly sequenced PCR products and therefore appear as heterozygous changes. *B*, Mutations segregating in two pedigrees with FEVR. Unaffected individuals (*unblackened*); affected individuals (*blackened*); individuals asymptomatic for FEVR (*blackened circle in square*). Family 1 shows the results of a restriction digest assay through use of *Hph*I, the recognition site of which is abolished by the mutation. The arrow indicates the undigested product present in affected individuals. Family 2 shows an SSCP trace (arrow indicates the aberrant shift). In family 2, an asterisk (*) indicates individuals affected by low bone mass. *C*, Protein-sequence alignment of human LRP5 (h) with homologues from human and other species: *Mus musculus* (m), *X. laevis* (x), *Drosophila melanogaster* ("arrow"), and *Anopheles gambiae str.* ("mosquito"). (GenBank accession numbers for all species appear in the "Electronic-Database Information" section.) Only 20 amino acid residues surrounding each mutation are shown. Conserved amino acid residues are highlighted. The positions of the missense mutations T173M, Y1168H, and C1361G are indicated. Both Y1168H and C1361G affect highly conserved amino acids, whereas T173M occurs at a less well-conserved residue.

A

```
LDL-R  390  KACKAVGSIAYLFFTNRHEVRKMTLD---RSEYTSLIPNLRNVVALDTEVASNRIYWSDLSQRMICS 453
LRP5    28  ----PAAASPLLLFANRRDVRLVDAGG-VKLESTIVVSGLEDAAAVDFQFSKGAVYWTDVSEEAIKQ  89
LRP5   338  -----AGAEEVLLLARRTDLRRISLDTPDFTDIVLQVDDIRHAIAIDYDPLEGYVYWTDDEVRAIRR 399
LRP5   642  ------VPEAFLVFTSRAAIHRISLET-NNNDVAIPLTGVKEASALDFDVSNNHIYWTDVSLKTISR 701
LRP5   943  ------PPTTFLLFSQKSAISRMIPDDQHSPDLILPLHGLRNVKAIDYDPLDKFIYWVDGRQNIKRA 1003

LDL-R  454  TQLDRAHGVSSYDTVISRDIQAPDGLAVDWIHSNIYWTDSVLGTVSVADTKGVKRKTLFREQGSKPR 520
LRP5    90  TYLN-QTGAAVQNVVIS-GLVSPDGLACDWVGKKLYWTDSETNRIEVANLNGTSRKVLFWQDLDQPR 154
LRP5   400  AYLD----GSGAQTLVNTEINDPDGIAVDWVARNLYWTDTGTDRIEVTRLNGTSRKILVSEDLDEPR 462
LRP5   702  AFMN----GSSVEHVVEFGLDYPEGMAVDWMGKNLYWADTGTNRIEVARLDGQFRQVLVWRDLDNPR 764
LRP5  1004  KDDGTQPFVLTSLSQGQNPDRQPHDLSIDIYSRTLFWTCEATNTINVHRLSGEAMGVVLRGDRDKPR 1070

LDL-R  521  AIVVDPVHGFMYWTDWGT-PAKIKKGGLNGVDIYSLVTENIQWPNGITLDLLSGRLYWVDSKLHSIS 586
LRP5   155  AIALDPAHGYMYWTDWGE-TPRIERAGMDGSTRKIIVDSDIYWPNGLTIDLEEQKLYWADAKLSFIH 220
LRP5   463  AIALHPVMGLMYWTDWGE-NPKIECANLDGQERRVLVNASLGWPNGLALDLQEGKLYWGDAKTDKIE 528
LRP5   765  SLALDPTKGYIYWTEWGG-KPRIVRAFMDGTNCMTLVDK-VGRANDLTIDYADQRLYWTDLDTNMIE 829
LRP5  1071  AIVVNAERGYLYFTNMQDRAAKIERAALDGTEREVLFTTGLIRPVALVVDNTLGKLFWVDADLKRIE 1137

LDL-R  587  SIDVNGGNRKTILEDEKRLAHPFSLAVFEDKVFWTDIINEAIFSANRLTGSDVNLLAENLLSPEDMV 653
LRP5   221  RANLDGSFRQKVVEG--SLTHPFALTLSGDTLYWTDWQTRSIHACNKRTGGKRKEILSALYSPMDIQ 285
LRP5   529  VINVDGTKRRTLLED--KLPHIFGFTLLGDFIYWTDWQRRSIERVHKVKAS-RDVIIDQLPDLMGLK 592
LRP5   830  SSNMLGQERVVIADD---LPHPFGLTQYSDYIYWTDWNLHSIERADKTSGRNRTLIQGHLDFVMDIL 893
LRP5  1138  SCDLSGANRLTLEDAN--IVQPLGLTILGKHLYWIDRQQQMIERVEKTTGDKRTRIQGRVAHLTGIH 1202

LDL-R  654  LFHQLTQPRGVNWCERTTLSNGGCQYLCLPAPQINPHSPKFTCACPDGMLLARDMRSCLTEAEAAVA 720
LRP5   286  VLSQERQPFFHTRCEE---DNGGCSHLCLLS----PSEPFYTCACPTGVQLQDNGRTCK-------- 337
LRP5   593  AVN-VAKVVGTNPCAD---RNGGCSHLCFFTP------HATRCGCPIGLELLSDMKTCI-------- 641
LRP5   894  VFHSSRQD-GLNDCMH---NNGQCGQLCLAIP------GGHRCGCASHYTLDPSSRNCS-------- 942
LRP5  1203  AVEEVSLEEFSAHPCAR--DNGGCSHICIAKG-----DGTPRCSCPVHLVLLQNLLTCG-------- 1254
```

B

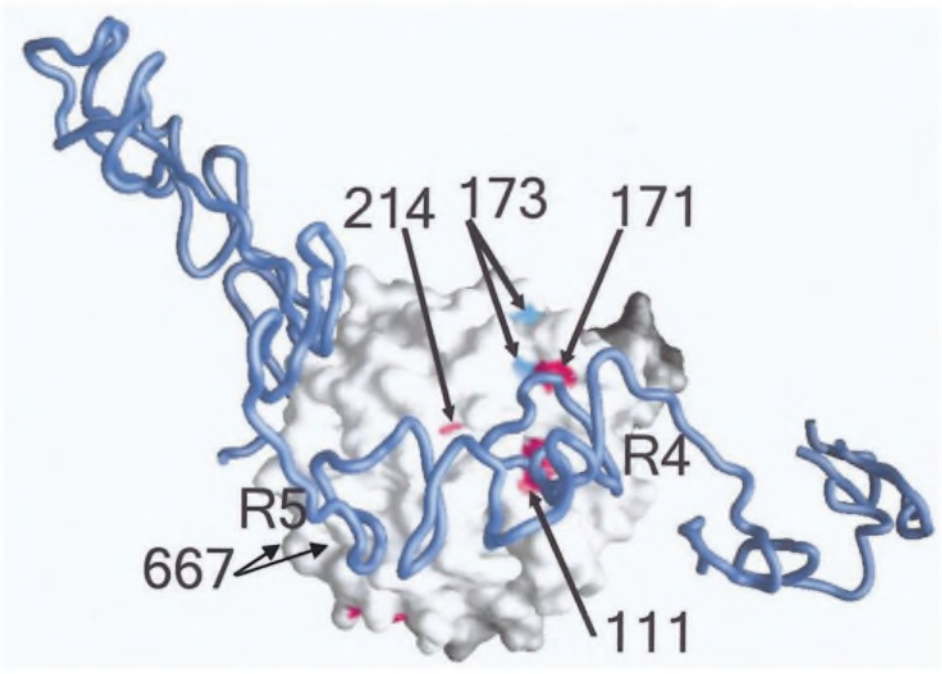

crystal structure of the YWTD-EGF domain of the LDL-R (Rudenko et al. 2002). To construct the model, the sequences of the four YWTD-EGF domains of LRP5 were aligned with the LDL-R sequence taken from the Protein Data Bank entry 1n7d (chain A), through use of the multiple-sequence-alignment program ClustalW (Chenna et al. 2003) (fig. 4*A*). The protein homology-modeling server Swiss-Model (Schwede et al. 2003) was then used to construct the model based on this alignment and the coordinates of the crystal structure of the LDL-R YWTD-EGF domain (1n7d chain A) (Rudenko et al. 2002) (fig. 4*B*). We used this model to map the missense mutations found in this study, as well as those missense mutations identified in patients with OPPG and high bone mass in other studies (Gong et al. 2001; Boyden et al. 2002; Little et al. 2002; Van Wesenbeeck et al. 2003), onto the three-dimensional structure of the LRP5 protein (fig. 4*B*).

Many of the mutations occur in the core of the protein and are likely to cause destabilization of the protein fold. This includes the FEVR mutation Y1168H from this study and some of the mutations shown to cause increased bone density (A242T and T253I) and OPPG (R570W). The remaining mutations occur at the protein surface (fig. 4*B*). It is less clear why mutations at these non–sequence-conserved positions (fig. 3*C*) would cause destabilization of the fold. However, six of the eight are clustered at one location on the protein surface (fig. 4*B*). It is interesting that all these mutations (T173M [causing FEVR] and D111Y, G171V, G171R, A214T, and A214V [causing high bone density]) are in the YWTD-EGF domain 1 of LRP5. Furthermore, all are in the same region that corresponds to the protein-protein–binding interface between modules R4 and R5 of the ligand-binding domain of LDL-R and the β-propeller domain of LDL-R (Rudenko et al. 2002). By analogy with LDL-R, it is possible that the surface region of the YWTD-EGF domains of LRP5 is also involved in protein-protein interactions and that mutating these nonconserved residues at the protein surface disrupts functionally important protein interactions.

Studies of LRP6 suggest that the first and second YWTD-EGF domains are required for LRP6 to interact functionally with the Wnt-frizzled complex, whereas the third and fourth YWTD-EGF repeats are required to bind Dickkopf-1 (Dkk-1), a secreted antagonist of the canonical Wnt-β-catenin pathway (Mao et al. 2001). A more recent study in *Xenopus* has also identified a new LRP6-interacting protein known as "Wise." Depending on its environment, Wise can act as both an activator and an inhibitor of Wnt signaling and interacts with the first and second YWTD-EGF repeats of LRP6, presumably by competing with the Wnt-frizzled complex (Itasaki et al. 2003). The high similarity between LRP5 and LRP6 suggests that equivalent interactions will occur in LRP5. Consistent with this notion, LRP5 has been shown to interact with different Wnt/frizzled complexes (Tamai et al. 2000; Semënov et al. 2001; Kato et al. 2002; Caricasole et al. 2003), although the binding sites have not been determined. Similarly, LRP5 has been shown to interact with Dkk-1 (Bafico et al. 2001; Caricasole et al. 2003), and in vitro studies have shown that the antagonizing effect of Dkk-1 on Wnt signaling is almost abolished when the wild-type LRP5 protein is replaced with one harboring the G171V mutation known to cause high bone mass (Boyden et al. 2002). Furthermore, LRP5 has also been reported to interact with other members of the Dickkopf (Dkk) family of proteins, Dkk-2 and Dkk-3 (Caricasole et al. 2003), and evidence suggests that these proteins, like the Wise protein, can function as either agonists or antagonists, depending on their cellular context (Wu et al. 2000; Mao and Niehrs 2003). These preliminary experiments indicate that comparable results can be obtained for both LRP5 and LRP6 and strengthen the conclusions, based on the modeling data, that the missense mutations disrupt a protein-binding site.

Expression studies have shown that *LRP5* and *LRP6* are widely expressed in both embryonic and adult tissues, including the retina (Brown et al. 1998; Hey et al. 1998; Kim et al. 1998). However, whereas mice lacking Lrp6 show a wide range of developmental defects in

Figure 4 Homology model of LRP5 YWTD-EGF domain 1. *A*, ClustalW alignment of the sequence from the YWTD-EGF domain, from LDL-R against the four YWTD-EGF domains found in LRP5. Amino acids are numbered in accordance with Swiss-Prot accession number P01130 (LDL-R) and GenBank accession number NP_002326 (LRP5). The amino acids highlighted in cyan correspond to the location of the T173M and Y1168H missense changes identified in the present study. The residues highlighted in pink correspond to the location of the missense mutations shown elsewhere to cause increased bone density (D111Y, G171V, G171R, A214T, A214V, A242T, and T253I) (Boyden et al. 2002; Little et al. 2002; Van Wesenbeeck et al. 2003) and OPPG (R570W, R494Q, and V667M) (Gong et al. 2001). The boxes correspond to the six YWTD-repeats present in the β-propeller module. The LDL-R and model LRP5 domain 1 share 37% sequence identity over 310 residues. *B*, Surface representation of the LRP5 YWTD-EGF domain 1. The model is based on the alignment shown in panel A. The location of mutations listed in panel A are highlighted on the surface in cyan and pink (numbers correspond to the amino acid residues). The blue backbone ribbon represents the ligand-binding domains R4 and R5 of LDL-R and illustrates how these interact with the propeller domain in LDL-R (Rudenko et al. 2002). Six of the missense mutations are located on the surface of the LRP5 YWTD-EGF domain 1 structure at a site corresponding to the protein-protein interface surface between the R4 and R5 ligand-binding domains and the propeller domain of LDL-R. (Figure prepared using GRASP [Nicholls et al. 1991])

multiple organs (Pinson et al. 2000), mice lacking Lrp5 have a restricted phenotype. Two groups have independently created mice with a targeted disruption of Lrp5 (Kato et al. 2002; Fujino et al. 2003), but it is surprising that these mice had different phenotypes. Kato et al. (2002) disrupted Lrp5 at amino acid 373 (exon 6), and immunohistochemistry showed that this allele resulted in the formation of a truncated polypeptide. The resultant homozygous mice had low bone mass and persistent embryonic eye vascularization, a phenotype similar to that observed in patients with OPPG. Fujino et al. (2003) disrupted Lrp5 at exon 18, but, this time, both immunoblotting and northern analysis indicated that the homozygous mice totally lacked Lrp5. These mice appeared normal, with no eye phenotype documented and only a very mild low-bone-mass phenotype, similar to osteoporosis, present in females aged >6 mo. These mice were, however, shown to have defects in their cholesterol metabolism and glucose-induced insulin secretion (Fujino et al. 2003). In both studies, the eyes of the heterozygotes appeared normal, but detailed analysis of the retinal vasculature by fluorescein angiography was not reported, so an FEVR phenotype cannot be ruled out.

In light of the results of the present study, we would have expected obligate OPPG carriers to have FEVR; it is surprising, therefore, that no eye defects have been reported. This is presumably a result of the subtle phenotype observed in some patients with FEVR (Ober et al. 1980). OPPG carriers have, however, been found to have reduced bone mass, when compared with age- and sex-matched control individuals (Gong et al. 2001). A closer inspection of affected members of family 2 who had the c4119–4120insC mutation showed that they, too, had signs of low bone mass (fig. 3*B*). Individual I:2 is osteoporotic. Her bone mineral density (BMD) is 60% of the normal sex-matched value and 65% of the age- and sex-matched value. No BMD figures were available for other affected family members, but their medical histories highlighted a large number of fractures. Individuals III:2 and III:3 have had multiple radius and humerus bone fractures since age 6 mo. Individual III:4 had a radial bone fracture at age 5 years, and individual I:3 has had six breaks in total (left wrist, right wrist, foot, femur, clavicle in two places, and right arm). These results suggest that patients with FEVR who have *LRP5* mutations show signs of osteoporosis, a clinical feature not previously noted in FEVR.

The microheterogeneity observed in this study highlights potential dangers in using multiple families for disease-gene refinement and identification. It is possible that one or both of these neighboring FEVR genes could have been excluded by combining haplotype data from families with mutations in both *FZD4* and *LRP5*, a worrying scenario for disease gene–mapping projects. Likewise, if the genetic analysis in family 1 had not excluded *FZD4* as the mutated gene in the family, the search for their mutation would have been abandoned, since it would have been presumed to lie outside the coding sequence of the gene. As a result, the second mutated gene at this locus might not have been identified.

In summary, we have shown that mutations in either *LRP5* or *FZD4*, two distinct genes within the *EVR1* locus, can cause FEVR. Together, these two loci account for 35% of FEVR cases in our patient series (15% *LRP5* and 20% *FZD4*), indicating that other unidentified FEVR genes may be a more significant cause of the disease than previously thought. The primary pathological process in FEVR is believed to be a premature arrest of retinal angiogenesis/vasculogenesis or retinal vascular differentiation, leading to incomplete vascularization of the peripheral retina. The implication of two components of the Wnt-signaling pathway in this disease process highlights the importance of its role in the development of the vasculature of the eye and, potentially, other organs.

Acknowledgments

We thank the families with FEVR, for their help in this study; The Wellcome Trust, for grants 069718/Z/02, 055145/Z/98, and 035535/Z/96; and the Jack Brockhoff Foundation, for financial support. K.Z. is supported by National Institutes of Health grants RO1EY14438, RO1EY14448, and GCRC M01-RR00064; the American Health Assistance Foundation; the Ruth and Milton Steinbach Fund; and the Ronald McDonald House Charities.

Electronic-Database Information

Accession numbers and URLs for data presented herein are as follows:

ClustalW, http://www.ebi.ac.uk/clustalw/

dbSNP, http://www.ncbi.nlm.nih.gov/SNP/ (for NCBI assay IDs ss16359666, ss16359667, ss16359668, ss16359669, ss16359670, ss16359671, ss16359672, ss16359673, ss16359674, ss16359675, ss16359676, ss16359677, ss16359678, and ss16359679)

GenBank, http://www.ncbi.nlm.nih.gov/Genbank/ (for hLRP5 [accession numbers NP_002326 and NM_002335], mLRP5 [accession number NP_032539], xLRP5 [accession number AAN09806], hLRP6 [accession number NP_002327], mLRP6 [accession number NP_032540] xLRP6 [accession number AAN09807], arrow [accession number AAF91072], mosquito [accession number EAA00402], and hLRP4 [accession number XP_035037])

Online Mendelian Inheritance in Man (OMIM), http://www.ncbi.nlm.nih.gov/Omim/ (for FEVR, *FZD4*, *LRP5*, OPPG, high bone mass, endosteal hyperostosis, and osteopetrosis)

Protein Data Bank, http://www.rcsb.org/pdb/

Swiss-Model, http://swissmodel.expasy.org/

Swiss-Prot, http://ca.expasy.org/sprot/sprot-top.html (for LDL-R [accession number P01130])

Wnt Gene Homepage, http://www.stanford.edu/~rnusse/wntwindow.html

References

Bafico A, Liu G, Yaniv A, Gazit A, Aaronson SA (2001) Novel mechanisms of Wnt signalling inhibition mediated by Dickkopf-1 interaction with LRP6/arrow. Nat Cell Biol 3:683–686

Benson WE (1995) Familial exudative vitreoretinopathy. Trans Am Ophthalmol Soc 93:473–521

Bieri S, Djordjevic JT, Daly NL, Smith R, Kroon PA (1995) Disulfide bridges of a cysteine-rich repeat of the LDL receptor ligand-binding domain. Biochemistry 34:13059–13065

Boyden LM, Mao J, Belsky J, Mitzner L, Farhi A, Mitnick MA, Wu D, Insogna K, Lifton RP (2002) High bone density due to a mutation in LDL-receptor-related protein 5. N Engl J Med 346:1513–1521

Brown SD, Twells RCJ, Hey PJ, Cox RD, Levy ER, Soderman AR, Metzker ML, Caskey CT, Todd JA, Hess JF (1998) Isolation and characterization of *LRP6*, a novel member of the low density lipoprotein receptor gene family. Biochem Biophys Res Commun 248:879–888

Caricasole A, Ferraro T, Iacovelli L, Barletta E, Caruso A, Melchiorri D, Terstappen GC, Nicoletti F (2003) Functional characterization of WNT7A signalling in PC12 cells. J Biol Chem 278:37024–37031

Chenna R, Sugawara H, Koike T, Lopez R, Gibson TJ, Higgins DG, Thompson JD (2003) Multiple sequence alignment with the Clustal series of programs. Nucleic Acids Res 31:3497–3500

Collins JS, Schwartz CE (2002) Detecting polymorphisms and mutations in candidate genes. Am J Hum Genet 71:1251–1252

De Crecchio G, Simonelli F, Nunziata G, Mazzeo S, Greco GM, Rinaldi E, Ventruto V, Ciccodicola A, Miano MG, Testa F, Curci A, D'Urso M, Rinaldi MM, Cavaliere ML, Castelluccio P (1998) Autosomal recessive familial exudative vitreoretinopathy: evidence for genetic heterogeneity. Clin Genet 54:315–320

Downey LM, Keen TJ, Roberts E, Mansfield DC, Bamashmus M, Inglehearn CF (2001) A new locus for autosomal dominant familial exudative vitreoretinopathy maps to chromosome 11p12-13. Am J Hum Genet 68:778–781

Fass D, Blacklow S, Kim PS, Berger JM (1997) Molecular basis of familial hypercholesterolaemia from structure of LDL receptor module. Nature 388:691–693

Frontali M, Stomeo C, Dallapiccola (1985) Osteoporosis-pseudoglioma syndrome: report of three affected sibs and an overview. Am J Med Genet 22:35–47

Fujino T, Asaba H, Kang M-J, Ikeda Y, Sone H, Takada S, Kim D-H, Ioka RX, Ono M, Tomoyori H, Okubo M, Murase T, Kamataki A, Yamamoto J, Magoori K, Takahashi S, Miyamoto Y, Oishi H, Nose M, Okazaki M, Usui S, Imaizumi K, Yanagisawa M, Sakai J, Yamamoto TT (2003) Low-density lipoprotein receptor-related protein 5 (LRP5) is essential for normal cholesterol metabolism and glucose-induced insulin secretion. Proc Natl Acad Sci USA 100:229–234

Gong Y, Slee RB, Fukai N, Rawadi G, Roman-Roman S, Reginato AM, Wang H, et al (2001) LDL receptor-related protein 5 (*LRP5*) affects bone accrual and eye development. Cell 107:513–523

Gow J, Oliver GL (1971) Familial exudative vitreoretinopathy: an expanded view. Arch Ophthalmol 86:150–155

Hey PJ, Twells RCJ, Phillips MS, Nakagawa Y, Brown SD, Kawaguchi Y, Cox R, Xie G, Dugan V, Hammond H, Metzker ML, Todd JA, Hess JF (1998) Cloning of a novel member of the low-density lipoprotein receptor family. Gene 216:103–111

Itasaki N, Jones CM, Mercurio S, Rowe A, Domingos PM, Smith JC, Krumlauf R (2003) Wise, a context-dependent activator and inhibitor of Wnt signalling. Development 130:4295–4305

Kato M, Patel MS, Levasseur R, Lobov I, Chang BH-J, Glass DA, Hartmann C, Li L, Hwang T-H, Brayton CF, Lang RA, Karsenty G, Chan L (2002) *Cbfa1*-independent decrease in osteoblast proliferation, osteopenia, and persistent embryonic eye vascularization in mice deficient in Lrp5, a Wnt coreceptor. J Cell Biol 157:303–314

Kim D-H, Inagaki Y, Suzuki T, Ioka RX, Yoshioka SZ, Magoori K, Kang M-J, Cho Y, Nakano AZ, Liu Q, Fujino T, Suzuki H, Sasano H, Yamamoto TT (1998) A new low density lipoprotein receptor related protein, LRP5, is expressed in hepatocytes and adrenal cortex, and recognizes apolipoprotein E. J Biochem 124:1072–1076

Kondo H, Hayashi H, Oshima K, Tahira T, Hayashi K (2003) Frizzled 4 gene (*FZD4*) mutations in patients with familial exudative vitreoretinopathy with variable expressivity. Br J Ophthalmol 87:1291–1295

Kondo H, Ohno K, Tahira T, Hayashi H, Oshima K, Hayashi K (2001) Delineation of the critical interval for the familial exudative vitreoretinopathy gene by linkage and haplotype analysis. Hum Genet 108:368–375

Laqua H (1980) Familial exudative vitreoretinopathy. Albrecht Von Graefes Arch Klin Exp Ophthalmol 213:121–133

Li Y, Fuhrmann C, Schwinger E, Gal A, Laqua H (1992*a*) The gene for autosomal dominant exudative vitreoretinopathy (Criswick-Schepens) on the long arm of chromosome 11. Am J Ophthalmol 113:712–713

Li Y, Müller B, Fuhrmann C, van Nouhuys CE, Laqua H, Humphries P, Schwinger E, Gal A (1992*b*) The autosomal dominant familial exudative vitreoretinopathy locus maps on 11q and is closely linked to D11S533. Am J Hum Genet 51:749–754

Little RD, Carulli JP, Del Mastro RG, Dupuis J, Osborne M, Folz C, Manning SP, et al (2002) A mutation in the LDL receptor–related protein 5 gene results in the autosomal dominant high–bone-mass trait. Am J Hum Genet 70:11–19

Mao B, Niehrs, C (2003) Kremen2 modulates Dickkopf2 activity during Wnt/LRP6 signalling. Gene 302:179–183

Mao B, Wu W, Li Y, Hoppe D, Stannek P, Glinka A, Niehrs C (2001) LDL-receptor-related protein 6 is a receptor for Dickkopf proteins. Nature 411:321–325

Müller B, Orth U, van Nouhuys CE, Duvigneau C, Fuhrmann C, Schwinger E, Laqua H, Gal A (1994) Mapping of the autosomal dominant exudative vitreoretinopathy locus

(*EVR1*) by multipoint linkage analysis in four families. Genomics 20:317–319

Nicholls A, Sharp KA, Honig B (1991) Protein folding and association: insights from the interfacial and thermodynamic properties of hydrocarbons. Proteins 11:281–296

Ober RR, Bird AC, Hamilton AM, Sehmi K (1980) Autosomal dominant exudative vitreoretinopathy. Br J Ophthalmol 64: 112–120

Pinson KI, Brennan J, Monkley S, Avery BJ, Skames WC (2000) An LDL receptor-related protein mediates Wnt signalling in mice. Nature 407:535–538

Plager DA, Orgel IK, Ellis FD, Hartzer M, Trese MT, Shastry BS (1992) X-linked recessive familial exudative vitreoretinopathy. Am J Ophthalmol 114:145–148

Price SM, Periam N, Humphries A, Woodruff G, Trembath RC (1996) Familial exudative vitreoretinopathy linked to D11S533 in a large Asian family with consanguinity. Ophthalmic Genet 17:53–57

Robitaille J, MacDonald MLE, Kaykas A, Sheldahi LC, Zeisler J, Dube MP, Zhang LH, Singaraja RR, Guernsey DL, Zheng B, Siebert LF, Hoskin-Mott A, Trese MT, Pimstone SN, Shastry BS, Moon RT, Hayden MR, Goldberg YP, Samuels ME (2002) Mutant frizzled-4 disrupts retinal angiogenesis in familial exudative vitreoretinopathy. Nat Genet 32:326–330

Rudenko G, Henry L, Henderson K, Ichtchenko K, Brown MS, Goldstein JL, Deisenhofer J (2002) Structure of the LDL receptor extracellular domain at endosomal pH. Science 298: 2353–2358

Schwede T, Kopp J, Guex N, Peitsch MC (2003) SWISS-MODEL: an automated protein homology-modelling server. Nucleic Acids Res 31:3381–3385

Semënov MV, Tamai K, Brott BK, Kühl M, Sokol S, He X (2001) Head inducer Dickkopf-1 is a ligand for Wnt coreceptor LRP6. Curr Biol 11:951–961

Shastry BS, Hejtmancik JF, Hiraoka M, Ibaraki N, Okubo Y, Okubo A, Han DP, Trese MT (2000) Linkage and candidate gene analysis of autosomal-dominant familial exudative vitreoretinopathy. Clin Genet 58:329–332

Shastry BS, Liu X, Hejtmancik JF, Plager DA, Trese MT (1997*a*) Evidence for genetic heterogeneity in X-linked familial exudative vitreoretinopathy. Genomics 44:247–248

Shastry BS, Trese MT (1997*b*) Familial exudative vitreoretinopathy: further evidence for genetic heterogeneity. Am J Med Genet 69:217–218

Tamai K, Semenov M, Kato Y, Spokony R, Liu C, Katsuyama Y, Hess F, Saint-Jeannet JP, He X (2000) LDL-receptor-related proteins in Wnt signal transduction. Nature 407:530–535

Toomes C, Bottomley HM, Scott S, Mackey DA, Craig JE, Appukuttan B, Stout JT, Zhang K, Black GCM, Fryer A, Downey LM, Inglehearn CF. Spectrum and frequency of *FZD4* mutations in familial exudative vitreoretinopathy (FEVR). Invest Ophthalmol Vis Sci (in press)

Toomes C, Downey LM, Bottomley HM, Scott S, Woodruff G, Trembath RC, Inglehearn CF (2004) Identification of a fourth locus (*EVR4*) for familial exudative vitreoretinopathy (FEVR). Mol Vis 10:37–42

Toomes C, Marchbank NJ, Mackey DA, Craig, JE, Newbury-Ecob, RA, Bennett, CP, Vize, CJ, Desai, SP, Black, GCM, Patel, N, Teimory, M, Markham, AF, Inglehearn, CF, Churchill, AJ (2001) Spectrum, frequency and penetrance of *OPA1* mutations in dominant optic atrophy. Hum Mol Genet 10: 1369–1378

van Nouhuys CE (1991) Signs, complications, and platelet aggregation in familial exudative vitreoretinopathy. Am J Ophthalmol 111:34–41

Van Wesenbeeck L, Cleiren E, Gram J, Beals RK, Bénichou O, Scopelliti D, Key L, Renton T, Bartels C, Gong Y, Warman ML, de Vernejoul M-C, Bollerslev J, Van Hul W (2003) Six novel missense mutations in the LDL receptor-related protein 5 (*LRP5*) gene in different conditions with an increased bone density. Am J Hum Genet 72:763–771

Wehrli M, Dougan ST, Caldwell K, O'Keefe L, Schwartz S, Vaizel-Ohayon D, Schejter E, Tomlinson A, DiNardo S (2000) Arrow encodes an LDL-receptor-related protein essential for Wingless signalling. Nature 407:527–530

Wu W, Glinka A, Delius H, Niehrs, C (2000) Mutual antagonism between Dickkopf1 and Dickkopf2 regulates Wnt/β-catenin signalling. Curr Biol 10:1611–1614